

Extraordinary light focusing and Fourier transform properties of gradient-index metalenses

Changbao Ma, Marco A. Escobar, and Zhaowei Liu*

Department of Electrical and Computer Engineering, University of California, San Diego, 9500 Gilman Drive, La Jolla, California 92093-0407, USA

(Received 3 October 2011; revised manuscript received 10 November 2011; published 28 November 2011)

We propose and demonstrate a new type of metalenses that are phase compensated by gradient index (GRIN) or inhomogeneous permittivity metamaterials. Both elliptically and hyperbolically dispersive GRIN metalenses for both internal and external focusing are studied. The requirements for the GRIN metalenses and the light focusing characteristics are analyzed and numerically verified. The GRIN metalenses can achieve super resolution and have ordinary or extraordinary Fourier transform functions, thus enabling exotic applications.

DOI: [10.1103/PhysRevB.84.195142](https://doi.org/10.1103/PhysRevB.84.195142)

PACS number(s): 78.67.Pt, 42.79.Bh, 42.79.Ry

I. INTRODUCTION

Lenses are pervasive in optical systems. The spatial resolution of a conventional lens is limited to about half the working wavelength $\sim \lambda_0/2$ due to the diffraction of light.¹ Immersion techniques are able to improve the resolution up to $\sim \lambda_0/(2n)$,^{2,3} such enhancement, however, is quite modest due to the low refractive index n of natural materials. It is worth mentioning that a number of super-resolution techniques, such as the stimulated emission-depletion microscopy,^{4,5} the single molecular/particle localization-based microscopy,^{6–8} and the structured illumination microscopy,^{9–11} have also been developed within the last two decades based on conventional optics. However, all these techniques have to deal with various limitations such as slow imaging speed, complex light illumination control and sample preparation, and additional numerical image reconstruction process. To achieve higher resolution from a lens point of view, a material that can support the propagation of light with higher wavevectors is needed. Artificial metamaterial may possess extraordinary material properties beyond the natural availabilities^{12–14} and thus have become an incomparable candidate for this purpose.

Various superlenses have been proposed and demonstrated with resolving power beyond the conventional diffraction limit within the last decade.^{15–24} Despite their super-resolving ability, such superlenses behave distinctly to their conventional counterpart. For instance, they cannot focus a plane wave due to the lack of phase compensation mechanism. Recently, two types of phase-compensated metamaterial lenses, i.e., the metamaterial immersion lens (MIL)²⁵ and the metalens,²⁶ were proposed by shaping or applying a plasmonic waveguide coupler array to a plasmonic metamaterial, respectively. While having super-resolving power, both the MIL and metalens can focus a plane wave, which is similar to a conventional optical lens. This plane-wave focusing property, i.e., Fourier transform, is a fundamental function of a lens and the basis of Fourier optics and optical data processing.

As is demonstrated, shaping a metamaterial for an MIL is similar to shaping a piece of glass for a conventional optical lens, in which the phase compensation for focusing is obtained by the geometry. From the point of view of transformation optics,^{27–29} the geometry variation can be transformed into the material space, resulting in inhomogeneous material properties in space, as is in a conventional gradient index (GRIN) lens.³⁰ In the past inhomogeneous metamaterials have attracted much

attention in cloaking, transformation optics, etc., and have also been shown to be able to focus optical beams and surface waves.^{28,29,31–36} Here we design new metalenses using gradient metamaterials, which we refer to as GRIN metalenses. The GRIN metalens possess super-resolving power as well as the Fourier transform capability.

II. THEORY AND ANALYSIS

The idea may be illustrated with a two-dimensional (2D) GRIN metalens. Although both the permittivity and permeability of metamaterials can be designed for novel devices and phenomena,^{12,32} it is prohibitively difficult to realize the tuning of the permeabilities of bulky metamaterials at the visible light frequencies. In this work we focus on plasmonic metamaterials, tuning only the permittivities because of their relatively low loss and availability of fabrication techniques for bulky materials.¹⁴ The dispersion of a 2D uniform plasmonic metamaterial $k_z^2/\epsilon_x + k_x^2/\epsilon_z = k_0^2$ may be either elliptic ($\epsilon'_x > 0$, $\epsilon'_z > 0$) or hyperbolic ($\epsilon'_x \cdot \epsilon'_z < 0$), with ϵ_x and ϵ_z being the complex permittivity of the metamaterial in the x (transverse) and z (propagation) directions, respectively; k_x and k_z being the wavevector in the x and z directions, respectively; k_0 being the wavevector in free space; and the prime representing the real part. We note that the materials with the combination of ($\epsilon'_x < 0$, $\epsilon'_z < 0$) are not considered because such materials do not support propagating waves. Varying the properties of a metamaterial in space, a GRIN metalens can be achieved, and its focus can be either inside or outside the metamaterial.

It is well known that a conventional GRIN lens requires a symmetric refractive-index profile with its maximum at the center for both internal and external focusing. The permittivity profiles (ϵ'_x , ϵ'_z) needed for a GRIN metalens, however, is not obvious due to the complexity resulting from the material anisotropy and possible positive or negative refraction at the lens/air interface. In the following we analyze the necessary types of permittivity profiles for a GRIN metalens and numerically verify the analysis using practical metamaterial designs.

Figure 1(a) shows the schematic one-period ray model of an internal-focusing GRIN metalens. The GRIN metalens can be modeled by discretizing the material into infinitesimally thin layers in the x direction, each of which may be considered as a uniform medium, as shown in Fig. 1(b) at an arbitrary location P on the ray trajectory AC in the converging region.

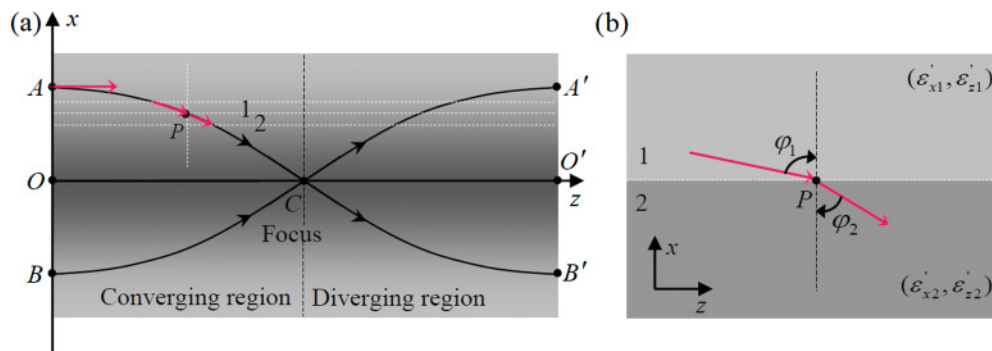


FIG. 1. (Color online) (a) Schematic ray model of a GRIN lens and its discretization in the x direction; (b) zoom-in view at a point P on a ray in the converging region.

The lens focusing problem is now simplified into a refraction problem at the interface between two adjacent anisotropic media. Assuming the material property variation is slow, it can be easily concluded that the refraction angle φ_2 should be always less than the incident angle φ_1 for all points on the ray trajectory before reaching the focus C . Giving anisotropic permittivities $(\varepsilon_{x1}, \varepsilon_{z1})$ and $(\varepsilon_{x2}, \varepsilon_{z2})$ to layers 1 and 2, respectively, the momentum conservation at the interface requires the following relation between φ_1 and φ_2 ,^{27,38}

$$\frac{\varepsilon'_{z1}}{\varepsilon_{x1}^2 \tan^2 \varphi_1} + \frac{1}{\varepsilon'_{x1}} = \frac{\varepsilon'_{z2}}{\varepsilon_{x2}^2 \tan^2 \varphi_2} + \frac{1}{\varepsilon'_{x2}}. \quad (1)$$

At point A , $\varphi_1 = 90^\circ$ and Eq. (1) is then reduced to

$$\tan^2 \varphi_2 = \frac{\varepsilon'_{x1} \varepsilon'_{z2}}{\varepsilon'_{x2} (\varepsilon'_{x2} - \varepsilon'_{x1})}. \quad (2)$$

In order to guarantee a solution of $\varphi_2 < 90^\circ$, the right-hand side of Eq. (2) needs to be larger than zero. Equation (2) indicates that ε'_x cannot be a constant; otherwise $\varphi_2 = 90^\circ$ and thus an incident plane wave will maintain its propagation direction without being altered to form a focus. We also notice the case that ε'_x has gradient but in which ε'_z keeps constant is extremely difficult to realize in practice; we therefore exclude the cases that either ε'_z or ε'_x is constant in the following study. Analyzing Eqs. (1) and (2), we obtain all the possible combinations of the symmetrical gradient profiles of ε'_x and ε'_z for the GRIN metalens to achieve internal focusing, which

we have summarized in Table I. If a GRIN metalens can focus inside the metamaterial, the outside focusing in air can be achieved by truncating the metamaterial in either the converging or diverging regions, which is determined by the positive (elliptically dispersive metamaterial) or negative refraction (hyperbolically dispersive metamaterial) experienced at the metamaterial/air interface. Another distinction between the hyperbolic and elliptic dispersions in GRIN metalenses is that a hyperbolically dispersive metamaterial with gradient ε'_x and ε'_z profiles that lead to internal divergence (no internal focus) still can bring light into an external focus through the negative refraction at the interface. All external focusing configurations are also included in Table I.

We emphasize that a ε'_z profile with a maximum at the center in case I-(ii) does not always result in internal focusing. Additional restriction

$$\dot{\varepsilon}'_z(x)/\dot{\varepsilon}'_x(x) < 2\varepsilon'_z(x)/\varepsilon'_x(x) \quad (3)$$

to the permittivity profiles, with the dot representing the derivative with respect to x , needs to be satisfied to guarantee the internal focusing. Because $\varepsilon'_x > 0$ and its maximum is at the center $\varepsilon'_{x2} > \varepsilon'_{x1}$ and $1/\varepsilon'_{x2} < 1/\varepsilon'_{x1}$, Eq. (1) thus becomes

$$\frac{\varepsilon'_{z1}}{\varepsilon_{x1}^2 \tan^2 \varphi_1} < \frac{\varepsilon'_{z2}}{\varepsilon_{x2}^2 \tan^2 \varphi_2}. \quad (4)$$

TABLE I. The conditions of symmetrical gradient anisotropic material properties for GRIN metalenses with internal and external focusing. Max and Min take the maximum and minimum, respectively; the dot atop $\varepsilon'_x(x)$ and $\varepsilon'_z(x)$ stands for the derivative with respect to x .

| Material properties | | | Requirements for gradient permittivity profile of | | Focus | | |
|---------------------|-----|---------------------|---|-------------------------------------|--|----------|--|
| Dispersion | | $\varepsilon'_x(x)$ | $\varepsilon'_z(x)$ | $\varepsilon'_x(x)$ | $\varepsilon'_z(x)$ | Internal | External |
| Elliptic | I | >0 | >0 | Max[$\varepsilon'_x(x)$] at $x=0$ | (i) Min[$\varepsilon'_z(x)$] at $x=0$ | Yes | Yes, truncate in the converging region |
| | | | | | (ii) Max[$\varepsilon'_z(x)$] at $x=0$, $\varepsilon'_z(x)/\varepsilon'_x(x) < 2\varepsilon'_z(x)/\varepsilon'_x(x)$ | | |
| Hyperbolic | II | >0 | <0 | Min[$\varepsilon'_x(x)$] at $x=0$ | Max[$\varepsilon'_z(x)$] at $x=0$, $\varepsilon'_z(x)/\varepsilon'_x(x) > 2\varepsilon'_z(x)/\varepsilon'_x(x)$ | Yes | Yes, truncate in the diverging region |
| | III | <0 | >0 | Max[$\varepsilon'_x(x)$] at $x=0$ | Min[$\varepsilon'_z(x)$] at $x=0$, $\varepsilon'_z(x)/\varepsilon'_x(x) < 2\varepsilon'_z(x)/\varepsilon'_x(x)$ | Yes | Yes, truncate in the diverging region |
| | IV | All others | | | | No | Yes |

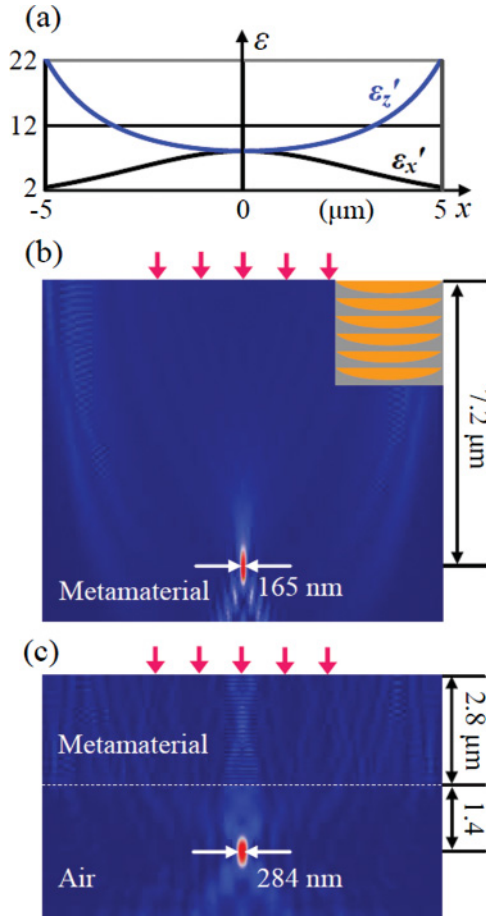


FIG. 2. (Color online) (a) Permittivity profiles of an elliptic GRIN metalens designed using multilayers of alternating silver (in gray) and TiO_2 (in yellow) with the thickness of silver varying symmetrically from the center to the edges. The silver-filling ratio ranges gradually from 0 at the center to 20% at both edges. The schematic geometry is shown as a legend in (b). Simulated electrical intensity (x component) distribution for (b) internal and (c) external focusing. $\lambda_0 = 660$ nm.

Because of the opposite monotonic property of $1/\varepsilon'_x(x)$ and $\varepsilon'_z(x)$ in the positive or negative x regions,

$$\frac{\varepsilon'_{z1}}{\varepsilon'^2_{x1}} > \frac{\varepsilon'_{z2}}{\varepsilon'^2_{x2}} \quad (5)$$

must be met to ensure $\varphi_2 < \varphi_1$. Rewriting this inequality using differential notations results in the additional restriction in inequality (3) to the ε'_z profile in case I-(ii). We note that the conventional GRIN lens is a subset of case I-(ii), with $\varepsilon'_x = \varepsilon'_z > 0$. The additional restrictions for other cases in Table I are similarly obtained.

III. SIMULATIONS AND VERIFICATION

Table I provides general guidance for choosing metamaterials in designing GRIN metalenses. An immediate rule for designing a GRIN metalens is that the type of the gradient profile of ε'_x should be looked after first. Once the ε'_x is chosen for the desired focusing behavior, the ε'_z profile is then determined by a specific metamaterial system. In the

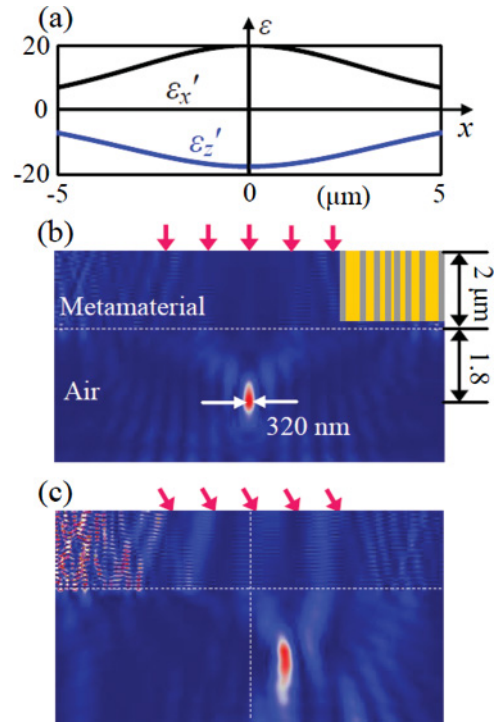


FIG. 3. (Color online) (a) Permittivity profiles of a hyperbolic GRIN metalens that has only external focusing designed using silver (in gray/dark gray) nanowires in an alumina (in yellow/light gray) background. The volume-filling ratio of silver varies symmetrically from 60% at the center to 30% at the edges. The schematic geometry is shown as a legend in the inset of (b). Simulated electrical intensity (x component) distribution for (b) normal and (c) tilted-incident plane wave. $\lambda_0 = 830$ nm.

following we illustrate the previous analyses for both internal- and external-focusing GRIN metalenses with cases I-(i), II, and a case in IV, which represent elliptic and hyperbolic internal-focusing GRIN metalenses and a hyperbolic metalens with only external focusing, respectively, using the commonly used multilayer³⁹ and nanowire⁴⁰ metamaterials. Note that we exclude cases I-(ii) and III in the demonstration because case I-(ii) is usually in the resonance regime and thus practically highly lossy; the type of metamaterials with $(\varepsilon'_x < 0, \varepsilon'_z > 0)$ in case III cannot support light propagation with wavevectors less than certain cut-off value.

Figure 2 shows an elliptic GRIN metalens with both internal and external focusing corresponding to case I-(i) in Table I. The permittivity profiles of an elliptic GRIN metalens for both internal and external focusing are the same; the only difference is their different lengths. This specific GRIN metalens is designed using Ag/ TiO_2 multilayers at 660 nm. The multilayers are orientated in the transverse (x) direction, and the thickness of Ag and thus the filling ratio varies symmetrically from $x = 0$ to the edges, as is schematically shown in the inset of Fig. 2(b). The permittivity profiles of the metalens are shown in Fig. 2(a), of which ε'_x is a squared hyperbolic secant profile,²⁹ which is used thereafter for all the other simulations. The material properties of Ag and TiO_2 , and all the other materials used thereafter, can be found in Ref. 41. Figure 2(b) shows the simulation of this elliptic GRIN metalens for internal focusing, which, and all other simulations

thereafter, was performed using the Comsol Multiphysics™. When it is truncated shorter, an external focus is attained, for which the simulation is shown in Fig. 2(c).

The diverging rays in a hyperbolic GRIN metalens can also achieve external focusing due to the negative refraction at the interface of metamaterial/air. Figure 3 shows such a hyperbolic GRIN metalens that only has an external focus, which is one of the “All others” cases in category IV in Table I. An incident normal plane wave is always diverged by such a hyperbolic metamaterial; no internal focus is formed. The metamaterial is designed using Ag nanowires oriented vertically in an alumina background, as is schematically shown in the inset of Fig. 3(b), of which the effective permittivity profiles are shown in Fig. 3(a). Figure 3(b) shows the simulation of this hyperbolic GRIN metalens illuminated with a normal plane wave at 830 nm; a focus is formed in air. In our MIL²⁵ and metalens²⁶ demonstration, the hyperbolic ones showed an abnormal focus-shifting behavior that is opposite to that in a conventional lens when the incident plane wave is tilted. However, the focus shifting behavior in air of this hyperbolic GRIN metalens is normal for tilted incident beam, as shown in Fig. 3(c), which is a result of the double negative refraction at the input and output metamaterial/air interfaces.

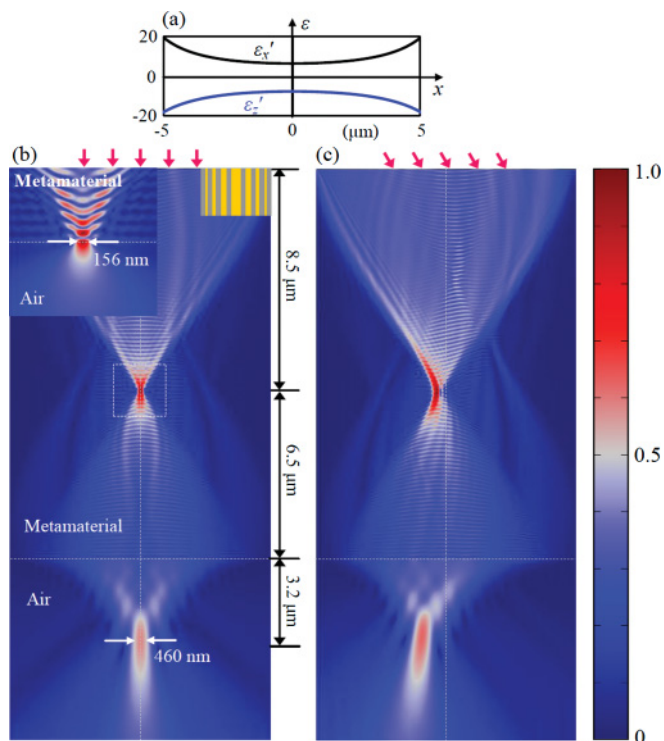


FIG. 4. (Color online) (a) Permittivity profiles of a hyperbolic GRIN metalens that has both internal and external focusing designed using silver (in gray/dark gray) nanowires in an alumina (in yellow/light gray) background. The volume-filling ratio of silver varies symmetrically from 30% at the center to 60% at the edges. The schematic geometry is shown as a legend in the right inset of (b). The left inset of (b) shows the zoom-in focus area when the metalens is truncated at its internal focal plane. Simulated electrical intensity (x component) distribution for (b) normal and (c) tilted-incident plane wave. $\lambda_0 = 830$ nm.

While the previous type of hyperbolic GRIN metalens can only have external focusing, a hyperbolic GRIN metalens may be designed to have both internal and external focusing. Figure 4 shows the permittivity profiles and the simulations of such a hyperbolic GRIN metalens in the category of case II in Table I. The metamaterial is designed using Ag nanowires oriented vertically in an alumina background at 830 nm, of which the permittivity profiles are shown in Fig. 4(a). Because a normal incident plane wave is converged by these permittivity profiles to form an internal focus, when it is truncated at the diverging region an external focus is formed due to the negative refraction at the metamaterial/air interface [see Fig. 4(b)]. When the incident beam is tilted, the internal focus is shifted anomalously to the side that is opposite to that in a conventional lens, as shown in Fig. 4(c), demonstrating its extraordinary Fourier transform function. The external focus is also shifted abnormally to the same side as the internal focus. The external focus is not directly formed by converging the incident plane wave but by a self-image of the internal focus, which explains the abnormal shifting originating from the hyperbolic dispersion.

IV. CONCLUSIONS AND DISCUSSIONS

As shown by the previous simulations, both the elliptical and hyperbolic GRIN metalenses can bring plane waves into a super-resolution focus inside the metamaterial. The super resolution originates from the exceptionally high effective refractive indices of the metamaterials. Although the resolution of the internal foci is still diffraction limited when compared with the wavelengths in the metamaterials, it is far beyond the achievable resolution by using conventional optical materials. For the same reason the GRIN metalenses can achieve much better resolution than conventional GRIN lenses. The resolution of an elliptically dispersive GRIN metalens is limited by the achievable $\epsilon'_z(0)$ [see Fig. 2(a)], which potentially can be further improved. Theoretically, the resolution of the hyperbolic GRIN metalens is unlimited due to the unlimited transverse-wavevector coverage; its practical resolution, however, is typically determined by the feature size and loss of the fabricated metamaterials.¹⁶ Although the GRIN metalenses are demonstrated at specific frequencies, they work off resonances and thus can work in a relatively wide band of frequencies around the design frequency.

When the metalens is truncated at a plane close to the internal focus, a super-resolution focus on the truncated surface in air is formed and can be accessed externally, as shown in the left inset of Fig. 4(b). Because the waves at the focus inside the metamaterial possess very high wavevectors, such waves become evanescent in air and decay rapidly away from the truncated surface. The focus in the air side composes plenty of evanescent wave components, so it is subdiffraction-limited.

It is worth noting that aperiodic metallic waveguide array, which falls into the category of the hyperbolic GRIN metalens presented in Fig. 4, was studied for deep-subwavelength focusing and steering of light,³⁵ indicating that $\lambda/100$ scale resolution could be achieved by the GRIN metalenses at longer wavelengths.³⁵ Our purpose of this work is to demonstrate the GRIN metalens concept, its designing rules, and exotic and unique focusing behaviors, which were focused on the

visible and near-infrared wavelengths. Without optimization, a resolution of $\lambda/6$ in air at the wavelength of 830 nm was easily achieved. Resolution better than $\lambda/100$ could be readily achieved in the GRIN metalenses at longer wavelengths. We finally note that the resolution of the GRIN metalenses could be further improved with the manipulation of polarization, for example, using radial polarization.⁴²

In conclusion we have theoretically derived the possible gradient permittivity combinations for GRIN metalenses with

internal and/or external focusing. They can achieve super resolution and focus a plane wave, thus can perform Fourier transform like a conventional lens. The near-field focus on the interface of a truncated GRIN metalens at its internal focal plane has the resolution beyond the diffraction limit. It can be easily accessed and utilized for many applications such as super-resolution imaging, information processing at the nanoscales, nanolithography, high density data storage, etc.

*Corresponding author: zhaowei@ece.ucsd.edu

¹E. Abbe, *Arch. Mikroskop. Anat.* **9**, 413 (1873).

²G. Kino, *Proc. SPIE* **3740**, 2 (1999).

³Q. Wu, G. D. Feke, R. D. Grober, and L. P. Ghislain, *Appl. Phys. Lett.* **75**, 4064 (1999).

⁴S. W. Hell and J. Wichmann, *Opt. Lett.* **19**, 780 (1994).

⁵M. Dyba and S. W. Hell, *Phys. Rev. Lett.* **88**, 163901 (2002).

⁶M. J. Rust, M. Bates, and X. Zhuang, *Nat. Methods.* **3**, 793 (2006).

⁷E. Betzig, G. H. Patterson, R. Sougrat, O. W. Lindwasser, S. Olenych, J. S. Bonifacino, M. W. Davidson, J. Lippincott-Schwartz, and H. F. Hess, *Science* **313**, 1642 (2006).

⁸D. Wu, Z. Liu, C. Sun, and X. Zhang, *Nano. Lett.* **8**, 1159 (2008).

⁹M. G. L. Gustafsson, *J. Microscopy* **198**, 82 (2000).

¹⁰L. Schermelleh, P. M. Carlton, S. Haase, L. Shao, L. Winoto, P. Kner, B. Burke, M. C. Cardoso, D. A. Agard, M. G. L. Gustafsson, H. Leonhardt, and J. W. Sedat, *Science* **320**, 1332 (2008).

¹¹F. Wei and Z. Liu, *Nano. Lett.* **10**, 2531 (2010).

¹²D. R. Smith, J. B. Pendry, and M. C. K. Wiltshire, *Science* **305**, 788 (2004).

¹³V. Shalaev, *Nat. Photon.* **1**, 41 (2007).

¹⁴J. Yao, Z. Liu, Y. Liu, Y. Wang, C. Sun, G. Bartal, A. M. Stacy, and X. Zhang, *Science* **321**, 930 (2008).

¹⁵J. B. Pendry, *Phys. Rev. Lett.* **85**, 3966 (2000).

¹⁶A. Grbic and G. V. Eleftheriades, *Phys. Rev. Lett.* **92**, 117403 (2004).

¹⁷N. Fang, H. Lee, C. Sun, and X. Zhang, *Science* **308**, 534 (2005).

¹⁸A. Salandrino and N. Engheta, *Phys. Rev. B* **74**, 075103 (2006).

¹⁹T. Taubner, D. Korobkin, Y. Urzhumov, G. Shvets, and R. Hillenbrand, *Science* **313**, 1595 (2006).

²⁰Z. Jacob, L. Alekseyev, and E. Narimanov, *Opt. Express* **14**, 8247 (2006).

²¹I. Smolyaninov, Y. Hung, and C. Davis, *Science* **315**, 1699 (2007).

²²Z. Liu, H. Lee, Y. Xiong, C. Sun, and X. Zhang, *Science* **315**, 1686 (2007).

²³Z. Liu, S. Durant, H. Lee, Y. Pikus, N. Fang, Y. Xiong, C. Sun, and X. Zhang, *Nano Lett.* **7**, 403 (2007).

²⁴X. Zhang and Z. Liu, *Nat. Mater.* **7**, 435 (2008).

²⁵C. Ma and Z. Liu, *Opt. Express* **18**, 4838 (2010).

²⁶C. Ma and Z. Liu, *Appl. Phys. Lett.* **96**, 183103 (2010).

²⁷J. B. Pendry, D. Schurig, and D. R. Smith, *Science* **312**, 1780 (2006).

²⁸V. Shalaev, *Science* **322**, 384 (2008).

²⁹U. Leonhardt, *Science* **312**, 1777 (2006).

³⁰C. Gómez-Reino, M. Pérez, and C. Bao, *Gradient-Index Optics: Fundamentals and Applications*, (Springer Verlag, New York, 2002).

³¹D. R. Smith, J. J. Mock, A. F. Starr, and D. Schurig, *Phys. Rev. E* **71**, 036609 (2005).

³²W. Cai, U. K. Chettiar, A. V. Kildishev, and V. M. Shalaev, *Nat. Photon.* **1**, 224 (2007).

³³J. Pendry, D. Schurig, and D. Smith, *Science* **312**, 1780 (2006).

³⁴U. Levy, M. Abashin, K. Ikeda, A. Krishnamoorthy, J. Cunningham, and Y. Fainman, *Phys. Rev. Lett.* **98**, 243901 (2007).

³⁵L. Verslegers, P. B. Catrysse, Z. Yu, and S. Fan, *Phys. Rev. Lett.* **103**, 033902 (2009).

³⁶M. Escobar, M. Berthome, C. Ma, and Z. Liu, *Appl. Opt.* **49**, 18 (2010).

³⁷T. M. Grzegorzczak, M. Nikku, X. Chen, B. I. Wu, and J. A. Kong, *IEEE Trans Microw. Theory Tech.* **53**, 1443 (2005).

³⁸Y. E. Kamach, E. N. Kozlovskii, and V. M. Ovchinnikov, *Sov. Phys.-Tech. Phys.* **22**, 1193 (1977).

³⁹S. A. Ramakrishna, J. B. Pendry, M. C. K. Wiltshire, and W. J. Stewart, *J. Mod. Opt.* **50**, 1419 (2003).

⁴⁰J. Pendry, A. J. Robbins, and W. J. Stewart, *J. Phys.-Condens. Matter* **10**, 4785 (1998).

⁴¹E. Palik and G. Ghosh, *Handbook of Optical Constants of Solids*, (Academic Press, San Diego, 1998).

⁴²R. Dorn, S. Quabis, and G. Lenchs, *Phys. Rev. Lett.* **91**, 233901 (2003).